Effect of a new non-cleavable substrate analog on wild-type and serine mutants in the signature sequence of adenylosuccinate lyase of *Bacillus subtilis* and *Homo sapiens*

SHARMILA SIVENDRAN AND ROBERTA F. COLMAN

Department of Chemistry and Biochemistry, University of Delaware, Newark, Delaware 19716, USA

(RECEIVED February 1, 2008; FINAL REVISION April 2, 2008; ACCEPTED April 2, 2008)

Abstract

Adenylosuccinate lyase (ASL) catalyzes two β-elimination reactions in purine biosynthesis, leading to the question of whether the two substrates occupy the same or different active sites. Kinetic studies of *Bacillus subtilis* and human ASL with a new substrate analog, adenosine phosphonobutyric acid, 2′(3′), 5′-diphosphate (APBADP), show that it acts as a competitive inhibitor with respect to either substrate ($K_I \sim 0.1$ μM), indicating that the two substrates occupy the same active site. Binding studies show that both the *B. subtilis* and human ASLs bind up to 4 mol of APBADP per mole of enzyme tetramer and that both enzymes exhibit cooperativity: negative for *B. subtilis* ASL and positive for human ASL. Mutant *B. subtilis* ASLs, with replacements for residues previously identified as critical for catalysis, bind the substrate analog similarly to wild-type ASL. Two serines in a flexible loop of ASL have been proposed to play roles in catalysis because they are close to the substrate in the crystal structure of *Escherichia coli* ASL. We have now mutated the corresponding serines to alanines in *B. subtilis* and human ASL to evaluate their involvement in enzyme function. Kinetic data reveal that human Ser^{289} and *B. subtilis* Ser^{262} and Ser^{263} are essential for catalysis, while the ability of these Ser mutants to bind APBADP suggests that they do not contribute to substrate affinity. Although these serines are not visible in the crystal structure of human adenylosuccinate lyase complexed with substrate or products (PDB #2VD6), they may be interacting with the active sites.

Keywords: adenylosuccinate lyase; substrate analog binding; site-directed mutagenesis

Supplemental material: see www.proteinscience.org

Reprint requests to: Roberta F. Colman, Department of Chemistry and Biochemistry, University of Delaware, Academy Street, Newark, DE 19716, USA; e-mail: rfcolman@udel.edu; fax: (302) 831-6335.

Abbreviations: AMP, adenosine monophosphate; ADP, adenosine diphosphate; SAMP, adenylosuccinate; SAICAR, succinylaminoimidazole carboxamide ribotide; AICAR, aminoimidazole carboxamide ribotide; APBADP, adenosine phosphonobutyric acid, 2′(3′), 5′-diphosphate; IMP, inosine monophosphate; CD, circular dichroism; TAPS, *N-tris*-(hydroxymethyl)methyl-3-aminopropanesulfonic acid; MES, 2-(*N*-morpholino)ethanesulfonic acid; HEPES, *N*-(2-hydroxyethyl)piperazine-N′-2-aminosulfonic acid; APBA, 2-amino-4-phosphonobutyric acid; *B. subtilis*, *Bacillus subtilis*; *H. sapiens*, *Homo sapiens*; *T. maritima*, *Thermatoga maritima*; *E. coli*, *Escherichia coli*.

Article published online ahead of print. Article and publication date are at http://www.proteinscience.org/cgi/doi/10.1110/ps.034777.108.

Adenylosuccinate lyase (ASL) (EC 4.3.2.2) catalyzes two reactions in the biosynthesis of purine nucleotides: the conversion of succinylaminoimidazole carboxamide ribotide (SAICAR) to aminoimidazole carboxamide ribotide (AICAR) in the purine de novo synthesis pathway, and the formation of adenosine monophosphate (AMP) from adenylosuccinate (SAMP) in the purine nucleotide cycle (Ratner 1972). The two reactions proceed by a uni–bi mechanism, where fumarate is removed by β-elimination via a general base–general acid mechanism. The general base abstracts a methylene proton from the carbon in the β-position relative to the leaving nitrogen, and the

 Copyright © 2008 The Protein Society

general acid donates a proton to the leaving nitrogen (Ratner 1972).

ASL deficiency is characterized by variable degrees of developmental delay, accompanied by autistic features and epileptic seizures (Van den Berghe and Jaeken 2001). This enzyme deficiency is diagnosed biochemically by the appearance in cerebrospinal fluid, urine, and plasma of succinylaminoimidazole carboxamide riboside (SAICA-riboside) and succinyladenosine (S-ado), the two dephosphorylated substrates of the enzyme (Van den Berghe and Jaeken 2001). In patients who are severely affected, the concentrations of these two compounds are close to one another, while in mildly affected patients, the SAICA-riboside concentration is in the same range, but the succinyladenosine concentration is much higher, resulting in S-Ado/SAICA-riboside ratios greater than 2 (Jaeken et al. 1998; Van den Berghe and Jaeken 2001). Therefore, there has been a question as to whether both reactions proceed at the same or different active sites. Synthesis of a substrate analog and evaluation of that analog as an inhibitor for both reactions could shed light on this question.

Point mutations of ASL result in inactive or less active enzymes, and the ability of these mutant enzymes to bind substrate is of interest (Spiegel et al. 2007). Since ASL is a one-substrate reaction in which adenylosuccinate is readily converted to products, it is difficult to measure binding of substrate using an *active* enzyme. However, a non-cleavable substrate analog could be used to compare the binding ability of mutant and normal wild-type (WT) enzymes.

The published crystal structure of the tetramer WT *Thermatoga maritima* adenylosuccinate lyase was obtained in the absence of substrate (Toth and Yeates 2000). Recently, crystal structures of *Escherichia coli* ASL inactive mutant H171A with bound SAMP and H171N with bound AMP + fumarate were published (Tsai et al. 2007), and the structures of human ASL in complex with AMP (PDB# 2J91) or with SAMP and AMP + fumarate (PDB# 2VD6) were determined. Previous affinity labeling and site-directed mutagenesis studies of the *Bacillus subtilis* ASL have indicated that His^{68} and His^{141} act as a general acid and general base, respectively (Lee et al. 1997, 1998, 1999). The recent *E. coli* mutant enzyme structure suggests that Ser^{295} (equivalent to *B. subtilis* Ser^{262} and human Ser^{289}) and His^{171} (equivalent to *B. subtilis* His^{141} and human His^{159}) act as the general base and general acid, respectively. Figure 1 shows the corresponding sequences of five bacterial and mammalian adenylosuccinate lyases in the region of *E. coli* Ser^{295}. The *E. coli* ASL structures indicate that there is a large conformational movement of the flexible loop region (including Ser^{295}) upon substrate binding, resulting in its closure over the active site. This loop region has not been visible in the other crystal structures. Although the overall sequence identity between the adenylosuccinate lyases

```
BACSU   FAKGQKGS262S263AMPHKRNPIGSE
THEMA   FRKGQRGS  S  AMPHKKNPITCE
ECOLI   TIAGEIGS295S296TMPHKVNPIDFE
MOUSE   FEKQQIGS  S  AMPYKRNPMRSE
HUMAN   FEKQQIGS289S290AMPYKRNPMRSE
                  **  *  .** * **   *
```

Figure 1. Amino acid sequence alignments of adenylosuccinate lyases from *B. subtilis*, *T. maritima*, *E. coli*, mouse, and human using ClustalW. The stars (*) designate amino acids which are completely conserved.

from these and other species is only ~12% (using ClustalW), the loop region is highly conserved and contains the signature sequence region for this superfamily of enzymes (Fig. 1). Ser^{295} of *E. coli* ASL was designated as being involved in catalysis because of its proximity to the substrate in the *E. coli* structure (Tsai et al. 2007).

In the present study we focus on the synthesis and evaluation of a new non-cleavable substrate analog to study the active sites of the two substrates of human and *B. subtilis* adenylosuccinate lyases. We also examine by mutagenesis the importance in catalysis of the two adjacent serine residues in the *B. subtilis* and human enzymes that are equivalent to *E. coli* Ser^{295} and Ser^{296}.

Results

Characterization of adenosine phosphonobutyric acid, 2′(3′), 5′-diphosphate (APBADP)

APBADP (Fig. 2, structure III) exhibits one peak at ~3 min on HPLC (in the solvent system and program described in the Supplemental material), as compared with ~40 min for 6-chloropurine riboside (Fig. 2, structure I) and ~10 min for 6-chloropurine riboside, 2′(3′), 5′-diphosphate (Fig. 2, structure II). The UV-Vis spectrum also exhibits one peak with a λ_{max} at 267 nm.

The proton NMR spectrum of APBADP is summarized in Supplemental Table S1 and the phosphorous NMR spectrum of APBADP is shown in Supplemental Figure S1. Chemical analysis of the organic phosphate content of APBADP shows the presence of 2.92 ± 0.21 mol of phosphorous per mole of compound, with the concentration determined from the A_{267nm} (ε = 19,900 M^{-1} cm^{-1}). These results are all consistent with the structure of adenosine phosphonobutyric acid, 2′(3′), 5′-diphosphate in Figure 2 (structure III).

Adenosine phosphonobutyric acid, 2′(3′), 5′-diphosphate (APBADP) studied as an inhibitor of B. subtilis *and human ASLs*

The substrate analog, APBADP, was tested at 20, 40, and 60 μM as a substrate with WT *B. subtilis* ASL, under standard conditions. No change in UV spectrum was observed

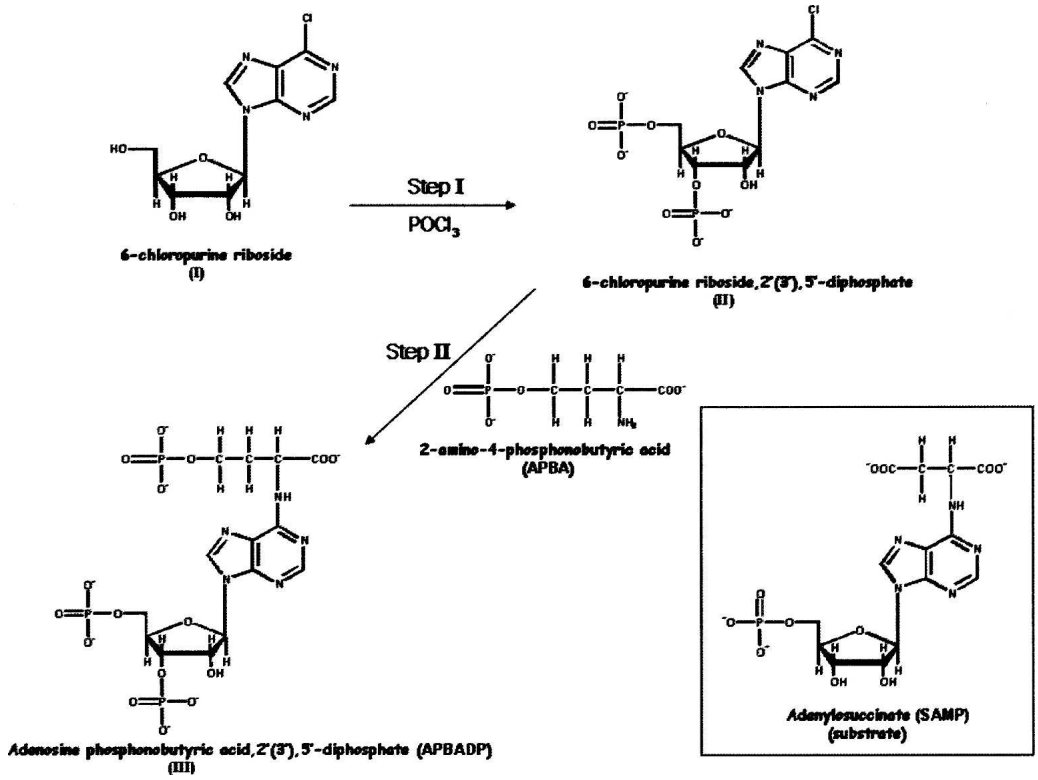

Figure 2. Synthesis of adenosine phosphonobutyric, 2′(3′), 5′-diposphate (APBADP). (*Inset*) For comparison, the structure of the substrate, adenylosuccinate (SAMP).

over 60 sec with 20 μL of 0.4 mg/mL WT enzyme. (In contrast, when this amount of enzyme was tested using adenylosuccinate, it gave a rate of ΔA_{282nm} of 0.15 min^{-1}). We conclude that, in contrast to 6-mercapto-9-β-D-ribofuranosylpurine 5′-phosphate (the 6-thio analog of adenylosuccinate), which is a substrate for yeast ASL (Hampton 1962) and for *B. subtilis* ASL (S. Sivendran and R.F. Colman, unpubl.), APBADP does not act as a substrate.

Instead, the APBADP was tested as an inhibitor of WT *B. subtilis* ASL at the constant concentrations of 0.25, 0.5, 0.75, and 1.0 μM, while the substrate SAMP was varied from 2 to 125 μM. The results are shown in Figure 3 and the kinetic constants are summarized in Table 1A. The pattern shown in Figure 3 is that of a classical competitive inhibitor. As the constant concentration of APBADP is increased, the K_m for SAMP increases from 2.0 μM in the absence of inhibitor to 17.1 μM in the presence of 1.0 μM inhibitor, while the V_{max} value does not change compared with the value measured in the absence of APBADP (1.26 μmol/min/mg). A K_I value can be calculated from each value of $K_{m(obs)}$ using the equation $K_{m(obs)} = K_m\,[1 + ([I]/K_I)]$ where K_m is the value obtained in the absence of APBADP, $K_{m(obs)}$ is the value measured in the presence of a known concentration of APBADP, and K_I is the apparent dissociation constant of an enzyme–APBADP complex. Alternatively, the K_I can be determined by rearranging the equation to $K_{m(obs)} = ((K_m/K_I)[I]) + K_m$, and plotting $K_{m(obs)}$ versus $[I]$, where K_I is equal to K_m/slope. The average K_I value for APBADP is 0.18 ± 0.04 μM.

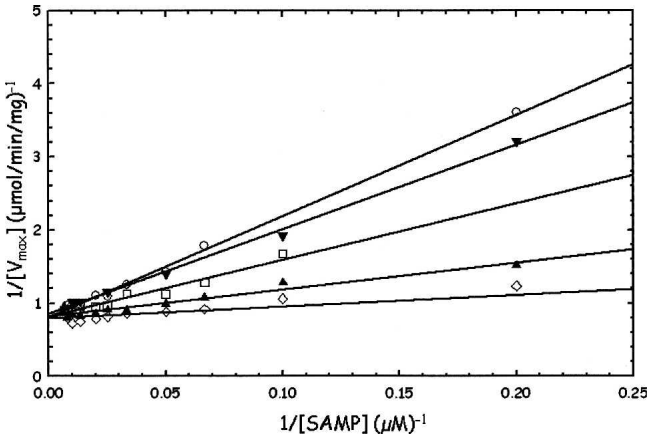

Figure 3. Determination of K_m for adenylosuccinate (SAMP) in the absence or presence of several constant concentrations of adenosine phosphonobutyric acid, 2′(3′), 5′-diphosphate (APBADP) using WT *B. subtilis* ASL. The following APBADP concentrations are shown: 0 μM (◇), 0.25 μM (▲), 0.5 μM (□), 0.75 μM (▼), and 1.0 μM (○).

Table 1. *WT* B. subtilis *and human ASL inhibition studies with adenosine phosphonobutyric acid, 2′(3′), 5′-diphosphate (APBADP)*

	SAMP[a]		SAICAR[b]	
APBADP	K_m (μM)	V_{max} (μmol/min/mg)	K_m (μM)	V_{max} (μmol/min/mg)
A. *B. subtilis* ASL				
Substrate + 0 μM	2.03 ± 0.46	1.26 ± 0.03	1.35 ± 0.21	1.29 ± 0.04
Substrate + 0.25 μM	4.19 ± 0.62	1.25 ± 0.03	—	—
Substrate + 0.50 μM	9.32 ± 0.99	1.22 ± 0.03	4.87 ± 1.61	1.37 ± 0.10
Substrate + 0.75 μM	14.1 ± 0.29	1.22 ± 0.05	—	—
Substrate + 1.00 μM	17.1 ± 0.54	1.24 ± 0.03	11.6 ± 3.55	1.39 ± 0.11
B. Human ASL				
Substrate ±0 μM	1.63 ± 0.28	3.23 ± 0.09	2.16 ± 0.39	8.05 ± 0.31
Substrate + 0.25 μM	5.48 ± 0.94	3.31 ± 0.14	—	—
Substrate + 0.50 μM	6.43 ± 0.59	3.13 ± 0.07	6.00 ± 0.85	9.56 ± 0.40
Substrate + 0.75 μM	16.1 ± 1.88	3.25 ± 0.13	—	—
Substrate + 1.00 μM	18.3 ± 1.74	3.30 ± 0.11	10.5 ± 1.33	9.54 ± 0.38

[a] SAMP activities were measured by the decrease in absorbance at 282 nm, and the K_m was determined by varying the SAMP concentration from 1 to 150 μM at each APBADP concentration. The K_I for APBADP as a competitive inhibitor is 0.18 ± 0.04 μM for *B. subtilis* ASL and 0.09 ± 0.04 μM for human ASL.
[b] SAICAR (succinylaminoimidazole carboxamide ribotide) activities were measured by the decrease in absorbance at 269 nm, and the K_m was determined by varying the SAICAR concentration from 1 to 150 μM concentration at each APBADP concentration. V_{max} was calculated by extrapolating to saturating concentrations of substrate. The K_I for APBADP as a competitive inhibitor was calculated as 0.16 ± 0.04 μM for *B. subtilis* ASL and 0.21 ± 0.08 μM for human ASL.

APBADP was also tested as a competitive inhibitor against SAICAR (Table 1A). As the concentration of APBADP is changed from 0 to 1.0 μM, K_m for SAICAR increases from 1.35 to 11.6 μM. However, the V_{max} does not decrease compared with V_{max} for SAICAR in the absence of APBADP (1.29 μmol/min/mg). Thus, APBADP also functions as a competitive inhibitor of *B. subtilis* ASL with respect to SAICAR as a substrate. The K_I value is 0.16 ± 0.04 μM.

Using WT human ASL, the substrate analog inhibitor, APBADP, was evaluated at constant concentrations of 0.25, 0.5. 0.75, and 1.0 μM as SAMP was varied from 1 to 150 μM (Table 1B). As the APBADP concentration is increased, the K_m for SAMP increases; in contrast, the V_{max} value does not change compared with the WT human ASL V_{max} value of 3.23 μmol/min/mg with SAMP as substrate. Thus, APBADP behaves as a competitive inhibitor with respect to SAMP for human ASL; the K_I value for APBADP is 0.09 ± 0.04 μM.

APBADP, at the constant concentrations of 0.5 and 1.0 μM, was also tested as a competitive inhibitor with respect to SAICAR using WT human ASL (Table 1B). As the concentration of APBADP is increased, the K_m for SAICAR increases, while the V_{max} value does not decrease. These results are consistent with APBADP functioning toward human ASL as a competitive inhibitor with respect to SAICAR. The K_I value is 0.21 ± 0.08 μM.

Direct binding of adenosine phosphonobutyric acid, 2′(3′), 5′-diphosphate (APBADP) to WT B. subtilis *ASL and human ASL*

The APBADP was tested for its ability to bind to WT *B. subtilis* ASL, with the results shown by the Scatchard plot in Figure 4, where r is the moles of APBADP bound per mole of enzyme subunit at a given $[APBADP]_{free}$, and n is the maximum number of moles of APBADP bound. A single binding site would be described by the Scatchard plot equation, $r/[ligand]_{free} = n/K_d - r/K_d$, and a plot of $r/[ligand]_{free}$ versus r would be linear. No single line describes all of this data (Fig. 4). The maximum number of moles of APBADP bound per mole of enzyme subunit is 0.96, or ~4 mol per mole of enzyme tetramer. As the r-value increases, the slope becomes lower, indicating a higher apparent K_d. The limits are shown by lines (A) and

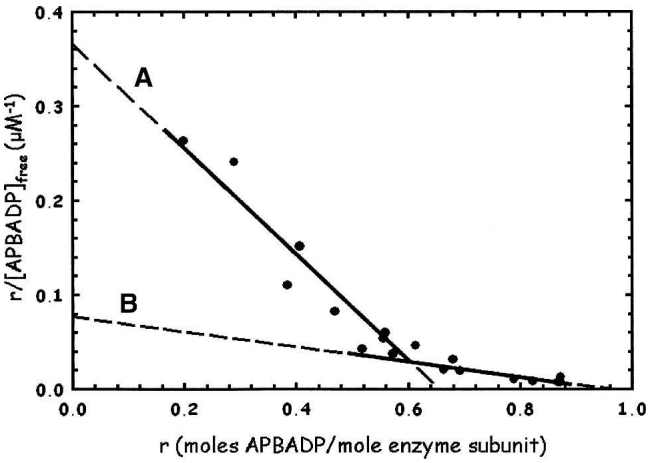

Figure 4. WT *B. subtilis* ASL binding studies with adenosine phosphonobutyric acid, 2′(3′), 5′-diphosphate (APBADP). The results are replotted as a Scatchard plot, described in Materials and Methods. Samples at 20 μM enzyme subunit were incubated with 5–120 μM total APBADP, and the free APBADP concentration was determined as described in Materials and Methods.

(B) in Figure 4, with line (A) giving $K_d = 1.78$ μM at values of r up to 0.5–0.6 and line (B) yielding $K_d = 12.6$ μM at $r = \sim 0.5$–0.96. This is an example of negative cooperativity, where binding to two active sites has the effect of weakening the binding to the other two active sites.

The inhibitor APBADP was also evaluated for binding to the human WT ASL, with the results shown as a Scatchard plot in Figure 5. The graph shows that, as the r values increase, the apparent K_d is decreased and binding is tighter. (If a line is drawn from a point on the curve, at about $r = 0.2 - 0.3$, to $r = 1.05$, the slope of the line would be lower than that of the limiting line, and K_d would be higher.) The limiting line (dashed) gives $K_d = 1.56$ μM with an n value of 1.05, showing that up to 1 mol of APBADP is bound per mole of enzyme subunit, or 4 mol per enzyme tetramer. This plot also exhibits cooperativity, but in this case it is positive cooperativity. This plot is similar to Scatchard plots reported for the binding of GTP by glutamate dehydrogenase (Frieden and Colman 1967), and for binding of various ligands by other enzymes (Koshland Jr. 1970). Binding at the first set of active sites appears to tighten affinity for the next set of active sites. Thus, both enzymes exhibit cooperativity in binding APBADP (positive for human, negative for *B. subtilis*), indicating that there is interaction between pairs of subunits.

One reason for synthesizing the non-cleavable substrate analog APBADP was to allow comparison of its binding by both normal active ASL and its mutants with lower or no activity. Table 2 demonstrates the usefulness of this compound, as the ability of WT and previously reported mutants of *B. subtilis* ASL to bind APBADP are

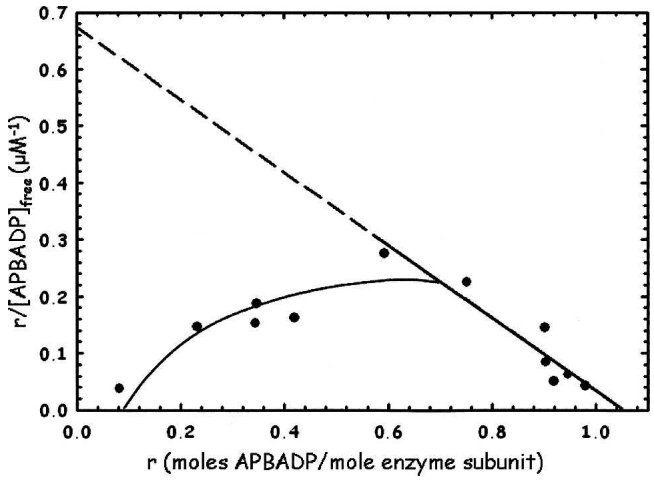

Figure 5. WT human ASL binding studies with adenosine phosphonobutyric acid, 2′(3′), 5′-diphosphate (APBADP). The results are replotted as a Scatchard plot, as described in Materials and Methods. Enzyme at 20 μM subunit concentration was incubated with 3–50 μM total APBADP, and the free APBADP concentration was determined as described in Materials and Methods.

Table 2. B. subtilis *mutant ASL binding studies with adenosine phosphonobutyric acid, 2′(3′), 5′-diphosphate*

Enzyme	Moles of APBADP bound per mole of enzyme subunit (r)
WT	0.55 ± 0.05
H141Q	0.65 ± 0.05
H68A	0.50 ± 0.12
H89Q	0.52 ± 0.07
H89R	0.51 ± 0.05
D69N	0.51 ± 0.03

The binding studies were conducted as described in Materials and Methods, with the total concentration of adenosine phosphonobutyric acid, 2′(3′), 5′-diphosphate at 30 μM and the total enzyme concentration at 19.9 μM for WT and mutant enzymes.

compared using a constant concentration of total APBADP (30 μM) and a constant total enzyme subunit concentration (19.9 μM). H141Q has been implicated in the active site by modification with the affinity label 6-BDB-TAMP (Lee et al. 1997) and by site-directed mutagenesis (Lee et al. 1999). Studies show that H141Q has no detectable activity, but binds radioactive SAMP with a K_d of 78 μM, indicating that His^{141} plays a role in catalysis rather than binding (Lee et al. 1999). However, since SAMP is cleaved by active enzyme, it was not possible to compare directly the binding of substrate by the mutant and WT enzyme (Lee et al. 1999). His^{68} has been implicated in the active site of *B. subtilis* ASL by modification by 2-BDB-TAMP and by site-directed mutagenesis (Lee et al. 1998). H68A has no detectable activity and a K_d of 52 μM with radioactive SAMP, indicating that His^{68} is important for catalysis and not binding since the affinity for substrate is decreased only 10- to 40-fold (Lee et al. 1998, 1999). H89Q has a specific activity of 0.0225 μmol/min/mg, so this enzyme could not be tested directly for its ability to bind adenylosuccinate, whereas H89R has a specific activity of only 0.0009 μmol/min/mg. Kinetic studies of His^{89} led to the postulate that it plays a role both in the binding of the AMP portion of the substrate and in correctly orienting the substrate for catalysis (Brosius and Colman 2000). D69N has a specific activity of 0.05 μmol/min/mg and only a modest twofold increase in K_m for SAMP, indicating that Asp^{69} is involved in catalysis and not in binding substrate (Sivendran et al. 2007). As shown in Table 2, all of these mutant enzymes bind the substrate analog APBADP as well as does WT enzyme. These results imply that His^{141}, His^{68}, His^{89}, and Asp^{69} are all important for catalysis, rather than for substrate binding.

Serine mutations in human and B. subtilis *ASL*

Serine residues 289 and 290 of the human ASL and serine residues 262 and 263 of *B. subtilis* ASL correspond to

E. coli ASL residues Ser^{295} and Ser^{296} (Fig. 1), based on sequence alignment using ClustalW. The serine residues of the *E. coli* ASL have been proposed to play a catalytic role on the basis of proximity to the substrate's succinyl moiety in the crystal structure of an inactive mutant *E. coli* ASL complexed with either adenylosuccinate or AMP + fumarate (Tsai et al. 2007). Human Ser^{289} and Ser^{290} and *B. subtilis* Ser^{262} and Ser^{263} were each mutated to alanine (to test for the role of the hydroxyl group at this position) or to histidine (to test whether imidazole is a catalytically acceptable replacement for serine's –OH group). Mutant enzymes were constructed, expressed, and purified as described in the Materials and Methods section. The purity of the enzyme preparations was established by single bands on polyacrylamide gel electrophoresis in the presence of SDS (data not shown). The WT and mutant human enzymes each exhibit single bands of subunit molecular weight of approximately 55,000, while the *B. subtilis* ASL mutants reveal a single subunit molecular weight band of 50,000.

Circular dichroism spectra of serine mutants

Circular dichroism (CD) spectra of the human and *B. subtilis* ASL serine mutants were determined (data not shown). For human ASL, the CD spectra of WT and the four mutant enzymes are superimposable, indicating that these mutants do not cause detectable changes in the secondary structure of the enzymes. For *B. subtilis* ASL, the CD spectra of WT and the Ser^{262} mutant enzymes are superimposable, and the Ser^{263} mutant enzymes show only minor differences in CD, indicating that there are no appreciable changes in the secondary structure of any of the mutants.

Molecular mass determination by light scattering of serine mutants of ASL

The masses of the serine mutant enzymes were determined at ~0.3 mg/mL concentration. The results are shown in Table 3, column 2. The human WT and mutant enzymes have similar masses around 229,000, indicating there is no difference in the enzyme's oligomeric structure. The *B. subtilis* WT and mutant ASLs have similar masses of about 195,000, showing that the mutant and WT enzymes exist predominantly as tetramers.

Kinetics and APBADP binding of human and B. subtilis *serine mutant ASL*

The activities of the same serine mutants of human and *B. subtilis* ASL were tested under standard conditions, with the results shown in Table 3, columns 3 and 4. Most of the human and *B. subtilis* serine mutant enzymes are inactive (when assayed using up to 25 times as much protein as for WT enzyme). Only human S290A ASL has detectable activity: The V_{max} is 0.4 μmol/min/mg, one-eighth of the V_{max} of the human WT enzyme, with a K_m for adenylosuccinate of 0.33 μM, compared with the human WT ASL K_m of 1.63 μM. These results indicate that Ser^{289} and Ser^{290} of human ASL and Ser^{262} and Ser^{263} of *B. subtilis* ASL may be involved in catalysis and/or binding.

The serine mutant human and *B. subtilis* ASL were also tested for their abilities to bind the non-cleavable

Table 3. *Kinetics, APBADP binding, and molecular masses of WT and Ser mutant adenylosuccinate lyases*

	Molecular masses (Da)[a]	V_{max} (μmol/min/mg)[b]	K_m (μM)[b]	k_{cat}/K_m (M^{-1} s^{-1})	Moles of APBADP bound per mole of enzyme subunit (r)[c]
Human					
WT	227,000 ± 19,000	3.23 ± 0.09	1.6 ± 0.3	1.72×10^6	0.68 ± 0.02
S289A	237,000 ± 12,000	0[d]	—		0.63 ± 0.08
S289H	227,000 ± 14,000	0[d]	—		0.49 ± 0.04
S290A	234,000 ± 3000	0.40 ± 0.02	0.3 ± 0.1	1.13×10^6	0.53 ± 0.07
S290H	221,000 ± 13,000	0[d]	—		0.58 ± 0.12
B. subtilis					
WT	191,000 ± 2000	1.32 ± 0.03	2.9 ± 0.5	3.82×10^5	0.55 ± 0.08
S262A	196,000 ± 5000	0[d]	—		0.52 ± 0.06
S262H	199,000 ± 12,000	0[d]	—		0.41 ± 0.03
S263A	197,000 ± 16,000	0[d]	—		0.40 ± 0.05
S263H	192,000 ± 6000	0[d]	—		0.47 ± 0.03

[a] Molecular weights were determined by light scattering on samples of 0.3 mg/mL at pH 7, 25°C.
[b] Activities were measured by the decrease in absorbance at 282 nm using SAMP as substrate. K_m was calculated by varying the SAMP concentration from 0.25 to 120 μM, and V_{max} was calculated by extrapolating to saturating concentration of substrate.
[c] All human and *B. subtilis* WT and Ser mutant ASL binding studies were conducted using 19.9 μM total enzyme concentration with 30 μM total APBADP concentration as described in Materials and Methods.
[d] The V_{max} of these mutants were below the detection limit, which was ~4.25×10^{-3} μmol/min/mg.

substrate analog APBADP. The results (Table 3, column 5) show that all of these enzymes bind comparable amounts of APBADP, indicating that the two adjacent serines do not contribute appreciably to substrate binding; rather, they must be involved in catalysis.

Discussion

This study identifies a new non-cleavable substrate analog inhibitor, adenosine phosphonobutyric acid, 2′(3′), 5′-diphosphate (APBADP), of *B. subtilis* and human adenylosuccinate lyase and uses it to determine if there are one or two distinguishable active sites for the two substrates of this enzyme. Adenosine phosphonobutyric acid, 2′(3′), 5′-diphosphate is a substrate analog with two additional phosphate groups (compared with the normal substrate, SAMP [Fig. 2, inset]): one on the ribose ring (either 2′ or 3′) and the other on the four-carbon chain. Previous studies on analogs of adenylosuccinate have shown that when the β-carboxyl is replaced by a phosphonate, the dianion of the phosphono group makes it a much better inhibitor (Brandt and Lowenstein 1978). Adenosine phosphonobutyric acid, 2′(3′), 5′-diphosphate (APBADP) is *not* a substrate for either WT *B. subtilis* or human ASL. This observation contrasts with the 6-thio analog of adenylosuccinate, which is cleaved (albeit slowly) by yeast (Hampton 1962) and *B. subtilis* ASL (S. Sivendran and R.F. Colman, unpubl.). The new substrate analog, APBADP, has a phosphono moiety instead of the β-carboxylate group of SAMP and an additional CH_2 as compared with the succinyl portion of SAMP (Fig. 2). The CH_2 β to the N^6 of APBADP is not activated by an adjacent carboxylate and (because of the greater length of the side chain of the purine) may not be well positioned near the enzyme's general base, thus accounting for the absence of cleavage of APBADP by the enzyme.

The effect of APBADP on the catalytic reactions of *B. subtilis* and human ASL is that of a classical competitive inhibitor: It increases the K_m for either SAMP or SAICAR as substrates without affecting the V_{max}. For *B. subtilis* ASL, the K_I for APBADP is 0.18 ± 0.04 μM when determined using SAMP as substrate, and 0.16 ± 0.04 μM using SAICAR as substrate. For human ASL, the K_I for APBADP is 0.09 ± 0.04 μM when calculated from the data with SAMP as substrate, and 0.21 ± 0.08 μM when determined using SAICAR as substrate. We conclude that both the substrates, SAMP and SAICAR, must be occupying the same active site since the K_I values for APBADP obtained from the two substrates are about the same within error in both *B. subtilis* and human ASL. This conclusion is supported by some of the mutant enzymes that have been studied, for which the change in the SAMP activity is essentially the same as the change in SAICAR activity (Kmoch et al. 2000; Sivendran et al. 2004). These results suggest that the different levels of the two dephosphorylated substrates detected in the extracellular fluids of some ASL-deficient patients are not due to the enzyme having two different active sites for the two substrates; instead, they may be due to disparate rates of transport of the two dephosphorylated substrates out of the cell, or to unequal rates of dephosphorylation of these compounds in patients.

Direct binding measurements of APBADP by *B. subtilis* and human ASL show that they bind 1 mol of APBADP per mole of enzyme subunit or 4 mol per mole of enzyme tetramer. Both enzymes exhibit cooperativity in binding the compound: one negative and the other positive cooperativity. This is the first functional evidence of cooperativity between subunits. Although this cooperative effect for ASL was not known before, another member of the fumarase superfamily of enzymes, argininosuccinate lyase, has shown negative cooperativity in kinetic and binding studies with its substrate arginine (Ratner 1972). Adenylosuccinate lyase is a tetramer; these binding studies suggest that both *B. subtilis* and human ASL function as a dimer of dimers in correspondence with the crystal structures (Toth and Yeates 2000; Tsai et al. 2007). In the recently reported crystal structure of human ASL (PDB# 2VD6), only two of the active sites have catalyzed the conversion of SAMP to AMP + fumarate, while the other two adenylosuccinate molecules are intact (Stenmark et al., in press). This observation is consistent with our studies and implies that the binding of the substrates to the first two sites is distinguishable from binding to the remaining two sites. We have recently, for human ASL, reexamined the dependence of velocity on adenylosuccinate over a wider concentration range than used previously, and *have* detected positive cooperativity in the kinetics (L. Ariyananda and R.F. Colman, unpubl.).

The dissociation constants for enzyme–inhibitor complex (K_d values) determined from the binding of APBADP to ASL are about 10 times higher than the K_I values calculated from the inhibition studies, although both experiments were conducted under the same general conditions. The difference could be due to the relatively high concentration of protein (20 μM enzyme subunits) used for the binding studies as compared with that used for the kinetic inhibition experiments (0.16 μM enzyme subunits). Although the K_d from the binding studies is higher than K_I, the direct binding experiments do allow comparisons to be made between WT and less active mutant enzymes measured under identical conditions. For *B. subtilis* mutant enzymes with substitutions for amino acids identified as critical for catalysis from previous affinity labeling and site-directed mutagenesis studies, the binding experiments demonstrate they bind APBADP to the same extent as the WT enzyme. The results imply

that these residues (His^{141}, His^{68}, His^{89}, and Asp^{69}) participate in catalysis, rather than substrate binding.

The recently published crystal structures of mutant *E. coli* ASL suggest that Ser^{295} is involved in catalysis because of its proximity to the β-carbon of the succinyl moiety of SAMP; it was proposed that Ser^{295} acts as a general base (Tsai et al. 2007). Also, *E. coli* Ser^{296} was observed within hydrogen bonding distance of the β-carboxylate of the succinyl portion of adenylosuccinate and thus was postulated to be involved in binding this part of the substrate. We mutated the equivalent serine residues in the *B. subtilis* and human enzymes to assess the effect of these residues on activity. Mutations of either serine in *B. subtilis* or human ASL yield a marked decrease in the catalytic activity. Only human S290A (corresponding to *E. coli* Ser^{296}) exhibits detectable catalytic activity: V_{max} is decreased eightfold, as compared with WT, with almost a fivefold decrease in K_m; however, the k_{cat}/K_m ratio of S290A enzyme is only decreased to 66% of the value for the WT enzyme, indicating that S290 is not required for activity. It appears that in human ASL, only the S289 enzyme is essential for catalysis, whereas in *B. subtilis* ASL both S262 and S263 are required.

The serine mutants of *B. subtilis* and human ASL are able to bind the substrate analog APBADP about as well as WT enzyme, implying that these serines are *not* directly involved in substrate binding. Although the *E. coli* mutant ASL structures suggest that Ser^{295} acts as the general base in the catalytic reaction because of its proximity to the C^{β}-proton of the substrate, the normally high pK of serine makes it an unlikely candidate. More likely is the possibility that once substrate is bound, these adjacent serines interact with other proximal amino acid residues to close the lid over the active site, thereby improving the environment for catalysis.

The loop region of adenylosuccinate lyase was suggested to be highly mobile (Toth and Yeates 2000) and has not been visualized in any of the crystal structures except the inactive *E. coli* mutant enzymes H171A and H171N in the presence of substrate and products. In the apo-ASL of *E. coli*, which lacks substrate and products, electron density was not observed for the residues 290–297 (*E. coli* numbering) in the loop (Tsai et al. 2007); therefore, it was proposed that the loop region becomes ordered in the presence of bound substrate. The *E. coli* mutant enzyme crystal structures in the presence of substrate and products demonstrate that there is a large conformational movement of the flexible loop region upon substrate binding, resulting in its closure over the active site. However, the recently deposited WT human ASL structure (PDB # 2VD6) in the presence of adenylosuccinate and products does *not* provide coordinates for the amino acids of this loop region; presumably, the loop in the human enzyme remains mobile even in the presence of the substrate, adenylosuccinate, or products, AMP + fumarate.

Figure 6A shows the structure of human ASL based on its determined crystal structure (PDB #2VD6), with an energy-minimized model of the loop region (residues

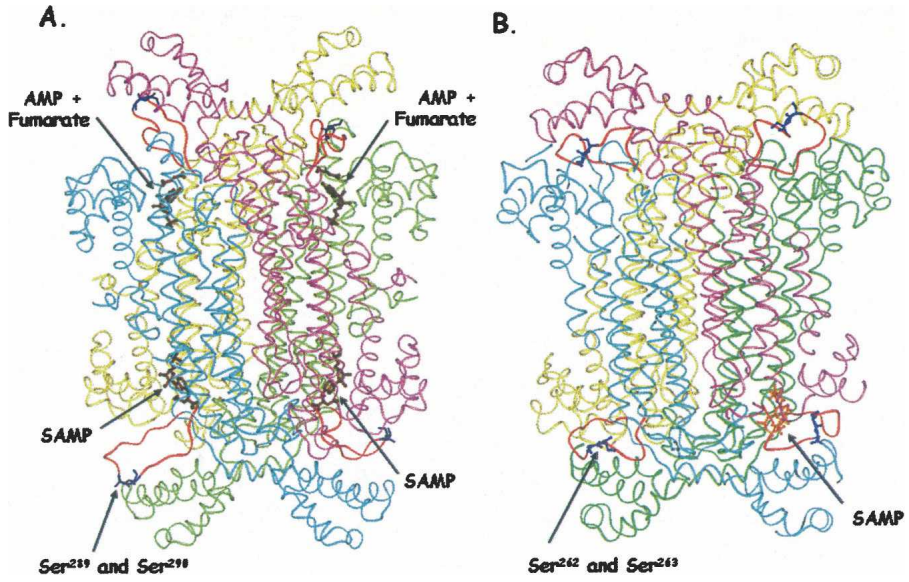

Figure 6. Human and *B. subtilis* ASL. (*A*) Human ASL (PDB# 2VD6), with the loop region modeled in. SAMP and AMP + fumarate are pictured in brown. (*B*) The *B. subtilis* ASL model was based on the *T. maritima* ASL structure (PDB# 1C3U) with the SAMP docked in one active site (shown in orange). The serine residues in human (S289 and S290) and *B. subtilis* (S262 and S263) are shown in blue on the orange loops. The active site in the *lower left* of panel *A* is enlarged in Figure 8.

282–293). The structure appears as a dimer of dimers with the cyan and pink subunits as one dimer and the green and yellow subunits as the other dimer. This figure also shows SAMP deeply imbedded in two active sites and AMP + fumarate bound to the other two active sites. The modeled loops (in orange) with the serine residues are far from the substrates and products. Figure 6B shows the homology model of *B. subtilis* ASL with the loops (also in orange), far from the active sites. The overall similarity of the two ASL structures, with the dimer of dimers feature, is apparent.

Structural alignment of the human and *E. coli* crystal structures (H171N with AMP + fumarate, and H171A with SAMP) is shown in Figure 7. Figure 7A shows the top left active site region from Figure 6A of the human ASL structure (PDB# 2VD6) containing AMP and fumarate, aligned with *E. coli* ASL containing AMP + fumarate (PDB# 2PTQ). Figure 7B shows the lower left active site region from Figure 6A of the human ASL structure (PDB# 2VD6) containing SAMP aligned with *E. coli* ASL containing SAMP (PDB# 2PTR). In Figure 7A,B the part of the human ASL structure for which there are atomic coordinates is shown in black, and the missing loop (which has been modeled) is pictured in orange. The entire *E. coli* ASL structure (shown in green) has been determined, but the corresponding loop region (from 287 to 303) is pictured in yellow. The figures demonstrate good structural alignment between the backbone of *E. coli* ASL residues 266–283 and 304–313 with the backbone of human ASL 260–277 and 298–307. Furthermore, the substrates of the *E. coli* and human enzymes superimpose. In contrast to most of the enzyme backbone, the loop regions are quite disparate, as shown in Figure 7A,B. The backbones of the two enzymes begin to deviate by human 279 and 296 (for which there *are* atomic coordinates) and *E. coli* 285 and 302. Clearly, the two serines in the human ASL loop are far from the substrate and products and quite distinct from those of *E. coli*. However, the human ASL loop is flexible, as indicated by the absence of electron density for residues 282–293, and it is possible that it could close over the active site so the human Ser^{289} and Ser^{290} become close to the positions of the *E. coli* Ser^{295} and Ser^{296}.

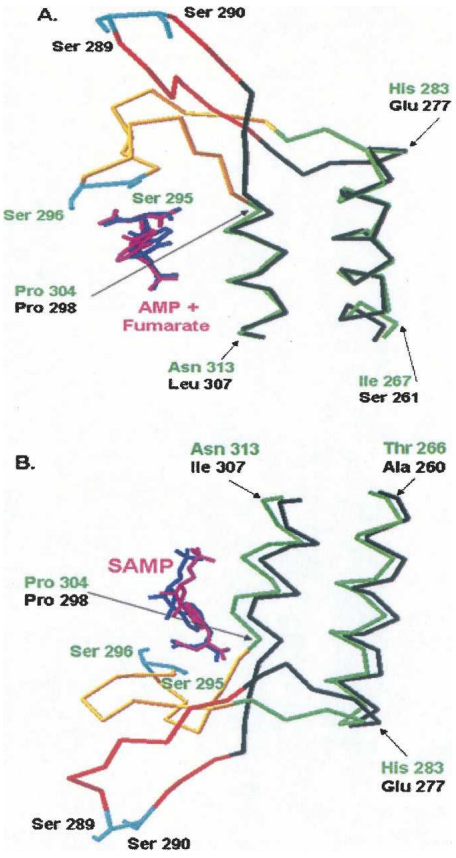

Figure 7. Structural alignment of human and *E. coli* ASL crystal structures. (*A*) *Top left* active site of human ASL structure of Figure 6A (which contains AMP + fumarate) with the *E. coli* ASL structure (PDB# 2PTQ). (*B*) *Lower left* active site of human ASL structure of Figure 6A (which contains SAMP) with *E. coli* ASL structure (PDB# 2PTR). The determined human ASL structure is shown in black with the missing loop region modeled and colored in orange (except for Ser^{289} and Ser^{290} which are shown in cyan). The *E. coli* ASL structure, which is completely determined, is shown in green with the established loop region colored in yellow. Ser^{295} and Ser^{296} are shown in cyan, for ease of comparison with the modeled human ASL loop region. SAMP, AMP, and fumarate from the human and *E. coli* structures are shown in pink and blue, respectively.

One of the human ASL active sites with SAMP bound (that on the lower left of Fig. 6A) is enlarged in Figure 8. The figure shows the three conserved histidines, His^{86}, His^{107}, and His^{159} (corresponding to *B. subtilis* residues His^{68}, His^{89}, and His^{141}), which are thought to be critical for catalysis on the basis of affinity labeling and site-directed mutagenesis studies. The three histidines are relatively close to the substrate, SAMP, although not sufficiently close for direct reaction. In contrast, Ser^{289} (equivalent to *B. subtilis* Ser^{262}) is extremely far (27.9 Å) from the C_β position of the succinyl moiety, where the *E. coli* crystal structure suggests it acts as the general base in catalysis. Ser^{290} (equivalent to *B. subtilis* Ser^{263}) is also far (22.8 Å) from the β-carboxylate of the succinyl group, where the *E. coli* structure suggests it plays a role in binding. The model of *B. subtilis* ASL also shows the loop region (containing Ser^{262} and Ser^{263}) far from the docked substrate.

The *E. coli* ASL may not be a good model for the active sites of the human or *B. subtilis* enzymes, since the structures of the loop region are so different. The sequence identity between *E. coli* and human ASLs is only 15.6%, and between *E. coli* and *B. subtilis* is but 21.1%, the lowest of all pairwise comparisons among ASLs. The same amino acids found to be catalytically important in *E. coli* ASL may have been recruited for different

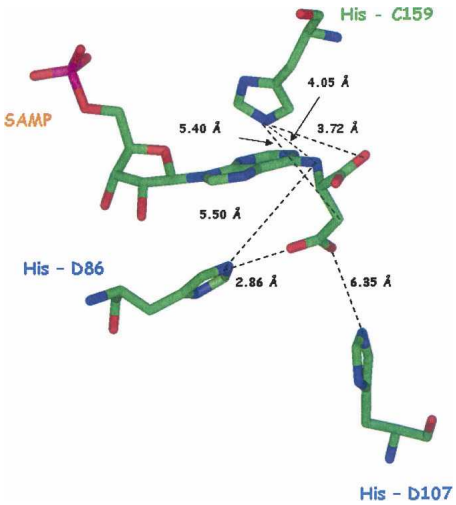

Figure 8. Enlargement of the active site of human ASL (PDB# 2VD6). The enlarged active site, which contains SAMP, is that shown in the *lower left* of Figure 6A.

functions in *B. subtilis* and human ASL. Alternatively, the inactive mutant *E. coli* ASL (H171A or H171N)-substrate crystalline structures may not reflect the actual situation in a WT enzyme complexed with substrate. An example of a mutant structure being different from the WT enzyme structure is δ-crystallin, for which the similar Ser^{283} of the loop region when mutated to alanine causes loss of enzyme activity and an altered conformation of the loop (Sampaleanu et al. 2002).

Another possible explanation (and perhaps the most likely) of the difference between the *E. coli* and human ASL crystal structures is that the human ASL structure shows the active sites with the substrates and products bound both before and after the transition state of the chemical reaction, and therefore these compounds are not positioned quite correctly for catalysis. This could explain why the histidine residues that are thought to be involved in catalysis are not *yet* close enough, and also why the loop is not ordered in the human ASL crystal structure. In the transition state, there may be small rearrangements so the substrate is better positioned to interact with the critical histidines and the enzyme may undergo a conformational change that either brings the loop region close to the substrate or sufficiently close to other residues to form a lid over the active site, thus sequestering the substrate. We *have* now established by mutagenesis that Ser^{289} of human ASL and Ser^{262} and Ser^{263} of *B. subtilis* ASL are essential for activity.

In summary, this study exploits a new substrate analog, APBADP, that is not cleaved by the enzyme. Inhibition studies with this substrate analog demonstrate that it acts as a classical competitive inhibitor with respect to SAMP and SAICAR of both the human and *B. subtilis* adenylosuccinate lyases; these results indicate that the two substrates occupy the same active site. Binding studies reveal that both human and *B. subtilis* adenylosuccinate lyases exhibit cooperativity in binding substrate. Mutagenesis of the conserved signature sequence loop region shows that serine residues are critical for catalysis, but not for binding substrate.

Materials and Methods

Materials

SAMP, SAICAR, HEPES, MES, TAPS, and imidazole were purchased from Sigma. Ni-NTA resin was purchased from Qiagen. Oligonucleotides for site-directed mutagenesis were obtained from Biosynthesis. 6-Chloropurine riboside was purchased from Aldrich. DL-2-Amino-4-phosphonobutyric acid was purchased from Lancaster. All other chemicals were of reagent grade.

Adenylosuccinate lyases of Bacillus subtilis *and* Homo sapiens

The pBHis plasmid encoding a 6-His tag on the N terminus of *B. subtilis* ASL was expressed in *E. coli* strain BL21(DE3), and the enzyme was purified to homogeneity using Qiagen nickel nitrilotriacetic acid-agarose (Redinbo et al. 1996; Lee et al. 1997). The purity of all enzyme preparations was evaluated using 12% polyacrylamide gels containing 0.1% sodium dodecyl sulfate (Laemmli 1970). The protein concentrations of *B. subtilis* ASL were determined from the absorbance at 280 nm using the $E^{1\%}_{280nm} = 10.6$ (Lee et al. 1997). Purified enzymes were stored at −80°C in 20 mM potassium phosphate, pH 7.0, containing 20 mM sodium chloride.

The pETN25HASL vector, which encodes a 6-His tag on the N terminus of the full-length human ASL, was expressed in *E. coli* Rosetta 2(DE3) pLysS cells, and the enzymes were purified to homogeneity using a Qiagen Ni-NTA column according to Lee and Colman (2007). The protein concentrations of human ASL were measured from the absorbance at 280 nm using $E^{1\%}_{280nm} = 14.1$, determined by the method of Groves et al. (1968). The purified enzymes were stored at −80°C in 50 mM potassium phosphate buffer, pH 7.0, containing 150 mM KCl, 1 mM DTT, 1 mM EDTA, and 10% glycerol, as described earlier (Lee and Colman 2007).

Kinetics of B. subtilis *and human adenylosuccinate lyases*

ASL activity toward SAMP was measured by the time-dependent decrease in absorbance at 282 nm using the difference extinction coefficient of 10,000 $M^{-1}cm^{-1}$ between SAMP and AMP. The *B. subtilis* WT and mutant enzymes were preincubated at a minimum concentration of 0.4 mg/mL in 20 mM potassium phosphate buffer, pH 7.0, containing 20 mM sodium chloride, for 30 min at 25°C prior to activity measurements (Palenchar and Colman 2003). The human WT and mutant enzymes were preincubated at a minimum concentration of 0.4 mg/mL in 50 mM potassium phosphate buffer, pH 7.0, containing 150 mM KCl, 1 mM EDTA, 1 mM DTT, and 10% glycerol, for 30 min at 25°C prior to activity measurements. Standard

assay conditions of 50 mM HEPES, pH 7.0 for *B. subtilis* (pH 7.4 for human ASL) at 25°C with 60 μM SAMP were used for the determination of specific activity, expressed as μmol/min/mg of enzyme used. The K_m for the WT and mutant enzymes was determined by varying the substrate concentration over the range 1–150 μM. The data were analyzed by *v* versus [S] with standard error estimates obtained from Sigma Plot software (SPSS, Inc.).

Synthesis of adenosine phosphonobutyric acid, 2′(3′), 5′-diphosphate (APBADP)

Adenosine phosphonobutyric acid, 2′(3′), 5′-diphosphate was synthesized by phosphorylation of 6-chloropurine riboside and then reaction of the product with 2-amino-4-phosphonobutyric acid (Fig. 2). The details of the synthesis are described in the Supplemental material.

Characterization of adenosine phosphonobutyric acid, 2′(3′), 5′-diphosphate (APBADP)

The proton and phosphorous NMR spectra of a 6 mM sample (III) in D_2O were obtained using a Bruker DRX400 spectrometer. The number of moles of organic phosphate per mole of compound was determined by the method described by Hess and Derr (1975) and Lanzetta et al. (1979), with slight modifications. Samples containing organic phosphorous (up to 10 nmol) were digested prior to phosphorous analysis. The sample was mixed with 20 μL of 10 N H_2SO_4, and the solutions were incubated in an aluminum foil closed tube for 2 h at 190°C. The samples, when cooled to room temperature, were analyzed for inorganic phosphate. Samples (150 μL) containing inorganic phosphate were mixed with 20 μL of 10 N H_2SO_4 and 800 μL of a fresh mixture of Malachite Green and ammonium molybdate (3:1), and the absorbance at 660 nm was read after 5 min. The standard curve was generated using 1–10 nmol of SAMP. IMP, ADP, and SAMP (5 nmol) were also tested as controls. The adenosine phosphonobutyric acid, 2′(3′), 5′-diphosphate was measured from 0.5 to 3 nmol.

Evaluation of inhibition of WT B. subtilis *and human ASL by adenosine phosphonobutyric acid, 2′(3′), 5′-diphosphate (APBADP)*

The substrate analog, APBADP (III), was tested as a substrate at 20, 40, and 60 μM concentrations with 20 μL of 0.4 mg/mL WT *B. subtilis* ASL under standard conditions in 50 mM HEPES, pH 7.0 at 25°C (but without SAMP). The K_m for the substrate, SAMP (2–150 μM), was determined in the absence or presence of several constant concentrations of APBADP (0.25–1.0 μM). The reaction was monitored by the time-dependent decrease in absorbance at 282 nm using the difference in extinction coefficient of 10,000 $M^{-1}cm^{-1}$ between SAMP and AMP. APBADP (at several constant concentrations) was also tested for its effect on the K_m of SAICAR (measured over a range of 2 to 125 μM), where the reaction of SAICAR to AICAR was monitored by the time-dependent decrease in absorbance at 269 nm using the difference in extinction coefficient of 700 $M^{-1}cm^{-1}$ between SAICAR and AICAR (Hampton 1962).

The substrate analog APBADP was also tested as a substrate at 20, 40, and 60 μM concentrations with 10 μL of 0.3 mg/mL WT human enzyme under standard conditions in 50 mM HEPES, pH 7.4 at 25°C (but without SAMP). The K_m for SAMP (1–150 μM) of human WT ASL was measured in the absence or presence of several constant concentrations of APBADP as described for *B. subtilis*. In this case, the kinetics were determined at 25°C in 50 mM HEPES pH 7.4 (Lee and Colman 2007). The K_m for SAICAR (2–150 μM) of the human ASL was also tested in the absence and presence of several constant concentrations of APBADP as described earlier for the *B. subtilis* enzyme.

Adenosine phosphonobutyric acid, 2′(3′), 5′-diphosphate (APBADP) binding studies

Binding experiments with *B. subtilis* and human WT ASL enzymes were carried out at 25°C by ultrafiltration, which is equivalent to equilibrium dialysis. Before loading the enzyme samples, the filtration units (Centricon YM-10 filtration units, Millipore) were prewashed with 1 mL of 50 mM HEPES, pH 7 for *B. subtilis* enzyme (pH 7.4 for human ASL) containing a particular concentration of APBADP. The 1 mL was filtered completely by centrifugation; this wash was repeated four times, until the absorbance of the eluate was the same as the solution that was applied. Samples at 20 μM enzyme subunit were incubated for 15 min with 5–120 μM (3–50 μM for human ASL) total APBADP in 0.5 mL for *B. subtilis* ASL before loading onto a Centricon YM-10 filtration unit and centrifuging at 6500 rpm for 20 min. Each binding experiment solution, containing enzyme and APBADP, was filtered in the same filtration device washed previously with the same concentration of total APBADP concentration. In the case of each enzyme-containing sample, the APBADP concentration in the filtrate was determined spectrophotometrically from $A_{267\ nm}$, and this was used to calculate the concentration of free APBADP. The enzyme-bound APBADP concentration was calculated from the difference between the total and free concentration of APBADP concentrations. The dissociation constant for APBADP with *B. subtilis* and human WT enzymes were determined using the Scatchard equation (Scatchard 1949), $r/[C]_{free} = n/K_d - r/K_d$, where *n* is the number of binding sites per enzyme subunit, *r* is the moles of bound compound per mole of enzyme subunit, and C_{free} is the concentration of free compound. The slope of $r/[C]_{free}$ versus *r* was used to calculate the dissociation constant (K_d). Various mutant *B. subtilis* and human ASLs were tested at a total concentration of 30 μM APBADP for their ability to bind the inhibitor.

Site-directed mutagenesis

Mutations to the pBHis plasmid (a gift from Dr. Jack E. Dixon, University of California, San Diego) containing *B. subtilis* ASL were constructed using the Stratagene QuikChange mutagenesis kit. The following oligonucleotides and their complements were used to generate the Ser^{262} and Ser^{263} mutant enzymes: (S262A): GGCAAAAGGGTGCATCTGCAATGCC; (S262H): GGCAAAAGGGTCATTCTGCAATGCCG; (S263A): GCAAAAGGGTTCAGCTGCAATGCCG; and (S263H): GCAAAAGGGTTCACATGCAATGCCGC. In each, the mutated codon is underlined. All mutations were confirmed by DNA sequencing, carried out at the University of Delaware Center for Agricultural Biotechnology using an ABI Prism model 377 DNA sequencer (PE Biosystems). The mutant *B. subtilis* ASLs were expressed in *E. coli* BL(21)DE3 and purified as for WT *B. subtilis* ASL.

Mutations to the pETN25HASL vector containing the full-length human ASL enzyme were constructed using the Stratagene QuikChange mutagenesis kit. The following oligonucleotides and their complements were used to generate the Ser^{289} and Ser^{290} mutant enzymes: (S289A): GCAGATTGGCGCAAGTGCG ATGCC; (S289H): CAGCAGATTGGCCATAGTGCGATGCCA; (S290A): GCAGATTGGCTCAGCTGCGATGCC; and (S290H): GCAGATTGGCTCACATGCGATGCCA. The mutant human ASLs were expressed in *E. coli* Rosetta 2(DE3) pLysS cells and purified as described for the WT human enzyme.

CD spectroscopy of human and B. subtilis *enzymes*

The secondary structure of the enzymes was assessed using a Jasco J-710 spectropolarimeter to measure ellipticity as a function of wavelength from 250 to 200 nm in 0.2-nm increments in a 0.1-cm cylindrical quartz cuvette. The WT and Ser *B. subtilis* and human mutant enzymes were preincubated at 0.4 mg/mL for 30 min at 25°C before measuring the spectra. Each sample was scanned five times and averaged, and the respective buffer spectrum was subtracted. The final protein concentration was determined by a dye-binding assay (Bio-Rad protein assay), based on the method of Bradford (1976), using a Bio-Rad 2550 RIA plate reader with a 600-nm filter. WT adenylosuccinate lyase was used as the protein standard. The mean molar ellipticity $[\theta]$ (deg cm^2 $dmol^{-1}$) was calculated from the equation $[\theta] = \theta/(10nCl)$, where θ is the measured ellipticity in millidegrees, C is the molar concentration of the enzyme subunits, l is the path length in centimeters, and n is the number of residues per subunit (437 including the 6-His tag for *B. subtilis* ASL and 503 for 6-His-tagged human ASL).

Determination of mass of B. subtilis *and human adenylosuccinate lyase serine mutants*

Light scattering was used to determine the masses of the WT and mutant enzymes. The samples (0.1–0.4 mg/mL concentration), in 20 mM potassium phosphate buffer, containing 20 mM NaCl, pH 7, for the *B. subtilis* enzymes and 50 mM potassium phosphate buffer, containing 150 mM KCl, 1 mM EDTA, 1 mM DTT, and 10% glycerol, pH 7, for the human enzymes, were measured at 25°C, using a miniDAWN laser photometer (Wyatt Technology Corp.). The data at the laser wavelength of 690 nm was analyzed using ASTRA software for Windows (Wyatt 1993). The protein concentrations were determined after collecting data using Bio-Rad (Bradford 1976) protein assays.

Homology modeling of adenylosuccinate lyase from human

A model of human adenylosuccinate lyase, which replaces the amino acid residues not seen in the crystal structure, was created using the SWISS-MODEL Protein Modeling program. The crystal structure of human adenylosuccinate lyase (PDB# 2VD6) was the template. Using ClustalW, the residues of the subunit from the amino acid sequence were aligned with each of the subunit residues observed in the crystal structure from the PDB, leaving the ''loop region'' without coordinates. The aligned sequences were submitted for modeling to the SWISS-MODEL Protein Modeling Server in the ''Alignment'' mode, giving an energy-minimized model (Guex and Peitsch 1997; Schwede et al. 2003; Arnold et al. 2006). The model of each subunit was then opened in the Swiss-Pdb Viewer and ''merged'' to form the tetramer.

In addition, the human ASL (PDB# 2VD6) and *E. coli* (PDB# 2PTR or PDB# 2PTQ) were structurally aligned in DeepView/Swiss-Pdb Viewer. The structures were aligned using the ''magic fit,'' ''iterative fit,'' and ''improve fit'' options for the structural alignment.

Electronic supplemental material

The synthesis and purification of adenosine phosphonobutyric acid, 2′(3′), 5′-diphosphate (APBADP) is described in the Materials and Methods section. The characterization of APBADP is presented in the Results section. The proton NMR results are summarized in Supplemental Table S1, and Supplemental Figure S1 shows the ^{31}P NMR spectrum of APBADP.

Acknowledgments

We thank Dr. Steve Bai for assistance with the NMR samples. This work was supported by NIH grant R01-DK 60504 and by a grant from Autism Speaks.

References

Arnold, R., Bordoli, L., Kopp, J., and Schwede, T. 2006. The Swiss MODEL workspace: A web-based environment for protein structure homology modeling. *Bioinformatics* **22:** 195–201.

Bradford, M.M. 1976. A rapid and sensitive method for the quantitation of microgram quantities of protein utilizing the principal of protein-dye binding. *Anal. Biochem.* **72:** 248–254.

Brandt, L.M. and Lowenstein, J.M. 1978. Inhibition of adenylosuccinase by adenylophosphonopropionate and related compound. *Biochemistry* **17:** 1365–1370.

Brosius, J.L. and Colman, R.F. 2000. A key role in catalysis for His^{89} of adenylosuccinate lyase of *Bacillus subtilis*. *Biochemistry* **39:** 13336–13343.

Frieden, C. and Colman, R.F. 1967. Glutamate dehydrogenase concentration as a determinant in the effect of purine nucleotides on enzymatic activity. *J. Biol. Chem.* **242:** 1705–1715.

Groves, W.E., Davis, J.F.C., and Sells, B.H. 1968. Spectrophotometric determination of microgram quantities of protein without nucleic acid interference. *Anal. Biochem.* **22:** 195–210.

Guex, N. and Peitsch, M.C. 1997. Swiss-MODEL and the Swiss-pdf viewer: An environment for comparative protein modeling. *Electrophoresis* **18:** 2714–2723.

Hampton, A. 1962. Studies of the action of adenylosuccinase with 6-thio analogues of adenylosuccinic acid. *J. Biol. Chem.* **237:** 529–533.

Hess, H.H. and Derr, J.E. 1975. Assay of inorganic and organic phosphorous in the 0.1–5 nanomole range. *Anal. Biochem.* **63:** 607–613.

Jaeken, J., Wadman, S.K., Duran, M., Van Sprang, F.J., Beemer, F.A., Holl, R.A., Theunissen, P.M., De Cock, P., Van den Bergh, F., Vincent, M.F., et al. 1998. Adenylo-succinase deficiency: An inborn error of purine nucleotide synthesis. *Eur. J. Pediatr.* **148:** 126–131.

Kmoch, S., Hartmannova, H., Stiburkova, B., Krijt, J., Zikanova, M., and Sebesta, I. 2000. Human adenylosuccinate lyase (ADSL), cloning and characterization of full-length cDNA and its isoform, gene structure and molecular basis for ADSL deficiency in six patients. *Hum. Mol. Genet.* **9:** 1501–1513.

Koshland Jr., D.E. 1970. The molecular basis for enzyme regulation. In *The enzymes*, 3rd ed., Vol. I (ed. P.D. Boyer), pp. 341–396. Academic Press, New York.

Laemmli, U.K. 1970. Cleavage of structural proteins during the assembly of the head of bacteriophage T4. *Nature* **227:** 680–685.

Lanzetta, P.A., Lawrence, J.A., Reinach, P.S., and Candia, O.A. 1979. An improved assay for nanomole amounts of inorganic phosphate. *Anal. Biochem.* **100:** 95–97.

Lee, P. and Colman, R.F. 2007. Expression, purification, and characterization of stable, recombinant human adenylosuccinate lyase. *Protein Expr. Purif.* **15:** 227–234.

Lee, T.T., Worby, C., Dixon, J.E., and Colman, D.F. 1997. Identification of His^{141} in the active site of *Bacillus subtilis* adenylosuccinate lyase by affinity labeling with 6-(4-bromo-2,3-dioxobutyl) thioadenosine 5′-monophosphate. *J. Biol. Chem.* **272:** 458–465.

Lee, T.T., Worby, C., Bao, Z.-Q., Dixon, J.E., and Colman, R.F. 1998. Implication of His^{68} in the substrate site of *Bacillus subtilis* adenylosuccinate lyase by mutagenesis and affinity labeling with 2-[(4-Bromo-2,3-dioxobutyl)thio]adenosine 5′-monophosphate. *Biochemistry* **37:** 8481–8489.

Lee, T.T., Worby, C., Bao, Z.-Q., Dixon, J.E., and Colman, R.F. 1999. His^{68} and His^{141} are critical contributors to the intersubunit catalytic site of adenylosuccinate lyase of *Bacillus subtilis*. *Biochemistry* **38:** 22–32.

Palenchar, J.B. and Colman, R.F. 2003. Characterization of a mutant *Bacillus subtilis* adenylosuccinate lyase equivalent to a mutant enzyme found in human adenylosuccinate lyase deficiency: Asparagine 276 plays an important structural role. *Biochemistry* **42:** 1831–1841.

Ratner, S. 1972. Argininosuccinases and adenylosuccinases. In *The enzymes*, 3rd ed., Vol. 7 (ed. P.D. Boyer), pp. 167–197. Academic Press, New York.

Redinbo, M.R., Eida, S.M., Stone, R.L., Dixon, J.E., and Yates, T.O. 1996. Crystallization and preliminary analysis of *Bacillus subtilis* adenylosuccinate lyase, an enzyme implicated in infantile autism. *Protein Sci.* **5:** 786–788.

Sampaleanu, L.M., Yu, B., and Howell, P.L. 2002. Mutational analysis of duck δ2 crystallin and the structure of an inactive mutant with bound substrate provide insight into the enzymatic mechanism of argininosuccinate lyase. *J. Biol. Chem.* **277:** 4166–4175.

Scatchard, G. 1949. The attractions of proteins for small molecules and ions. *Ann. N. Y. Acad. Sci.* **51:** 660–672.

Schwede, T., Kopp, J., Guex, N., and Peitsch, M.C. 2003. Swiss-MODEL: An automated protein homology-modeling server. *Nucleic Acids Res.* **31:** 3381–3385.

Sivendran, S., Patterson, D., Spiegel, E., McGowen, I., Cowley, D., and Colman, R.F. 2004. Two novel mutant human adenylosuccinate lyases associated with autism and characterization of the equivalent mutant *Bacillus subtilis* ASL. *J. Biol. Chem.* **279:** 53789–53797.

Sivendran, S., Segall, M.L., Rancy, P.C., and Colman, R.F. 2007. Effect of Asp^{69} and Arg^{310} on the pK of His^{68}, a key catalytic residue of adenylosuccinate lyase. *Protein Sci.* **16:** 1700–1707.

Spiegel, E.K., Colman, R.F., and Patterson, D. 2007. Adenylosuccinate lyase deficiency (a review). *Mol. Genet. Metab.* **89:** 19–31.

Stenmark, P., Moche, M., Arrowsmith, C., Berglund, H., Busam, R., Collins, R., Dahlgren, L.G., Edwards, A., Flodin, S., Flores, A., et al. Human adenylosuccinate lyase in complex with its substrate N6-(1,2-dicarboxyethyl)-AMP, and its products AMP and fumarate. *RCSB Protein Data Bank* (in press). doi: 1032210/pdb2vd6/pdb.

Toth, E.A. and Yeates, T.O. 2000. The structure of adenylosuccinate lyase, an enzyme with dual activity in the de novo purine biosynthetic pathway. *Structure* **8:** 163–174.

Tsai, M., Koo, J., Yip, P., Colman, R.F., Segall, M.L., and Howell, P.L. 2007. Substrate and product complexes of *E. coli* adenylosuccinate lyase provide new insights into the enzymatic mechanism. *J. Mol. Biol.* **370:** 541–554.

Van den Berghe, G. and Jaeken, J. 2001. Adenylossuccinate lyase deficiency. In *The metabolic and molecular basis of inherited diseases*, 8th ed., Vol. II (eds. C.R. Scriver et al.), pp. 2653–2662. McGraw-Hill, New York.

Wyatt, P.J. 1993. Light scattering and the absolute characterization of macromolecules. *Anal. Chim. Acta* **272:** 1–40.